RAA 2015 Vol. **15** No. **8**, 1275–1281 doi: 10.1088/1674–4527/15/8/012
http://www.raa-journal.org *http://www.iop.org/journals/raa*

***R**esearch in*
***A**stronomy and*
***A**strophysics*

A search for Mg-poor stars using LAMOST survey data

Qian-Fan Xing[1,2], Gang Zhao[1], Yong Zhang[3], Yong-Hui Hou[3], Yue-Fei Wang[3] and Yue Wu[1]

[1] Key Laboratory of Optical Astronomy, National Astronomical Observatories, Chinese Academy of Sciences, Beijing 100012, China; *qfxing@nao.cas.cn; gzhao@nao.cas.cn*
[2] University of Chinese Academy of Sciences, Beijing 100049, China
[3] Nanjing Institute of Astronomical Optics & Technology, National Astronomical Observatories, Chinese Academy of Sciences, Nanjing 210042, China

Received 2015 April 1; accepted 2015 May 20

Abstract Most Galactic metal-poor stars exhibit enhanced α-abundances (e.g. [Mg/Fe] $\sim +0.4$) according to previous studies of stellar chemical compositions. However, a handful of metal-poor stars with large deficiencies in Mg (e.g. [Mg/Fe] ~ -0.2) show severe departures from this α-enhancement trend. The sub-solar [Mg/Fe] ratios of these anomalous stars indicate that they possess different chemical enrichment histories than the majority of Galactic metal-poor stars. In previous work, we presented a method to select Mg-poor metal-poor stars from low-resolution SDSS spectra based on a spectral matching technique. In this paper, a similar method is applied to low-resolution ($R \sim 1800$) LAMOST spectra. Stellar [Mg/Fe] abundances are determined by using stellar parameters delivered by the LAMOST Data Release 2 catalog. From a sample of $\sim 60\,000$ stars with atmospheric parameters in the range $T_{\rm eff}$ = [5500, 6500] K and [Fe/H] = [−2.4, +0.5], we select 15 candidate Mg-poor metal-poor stars.

Key words: methods: data analysis — stars: abundance — stars: atmospheres

1 INTRODUCTION

The unique abundance patterns of the α-elements (O, Mg, Si, Ca and Ti) exhibited by the Galactic halo and disk reveal an important role that environment plays in Galactic chemical evolution. Most observed metal-poor stars typically exhibit enhanced Mg-element abundance [Mg/Fe] $\sim +0.4$ (Edvardsson et al. 1993; McWilliam 1997). The enhanced [Mg/Fe] ratios observed in metal-poor stars are due to the time delay between Type II and Ia supernovae according to the scenario given by Tinsley (1979). The lifetimes of Type Ia supernova (SN Ia) progenitors are much longer than those of Type II supernova (SN II) progenitors. From the resulting explosions of high-mass ($> 8M_\odot$) and short-lived stars, SNe II contributed the main chemical materials that enriched α-elements in the interstellar medium (ISM) at the early stage of the Galaxy. The generations of stars born out of this polluted ISM thus show enhancement of Mg with respect to Fe.

However, some Mg-poor stars have been confirmed with [Mg/Fe] ratios that are quite different from the enhancement trends of metal-poor stars. The existence of Mg-poor stars was first claimed by Carney et al. (1997), based on high-resolution spectra. More such Mg-poor stars were discovered by a number of later studies (King 1997; Preston & Sneden 2000). All of these abnormal stars possess [Mg/Fe] below the solar ratio in a low metallicity range, suggesting that a considerable scatter in the Mg abundance may exist in this metallicity range. Hence, several studies have been trying to investigate stars in the solar neighborhood that are outliers in terms of [Mg/Fe]. Stephens & Boesgaard (2002) proposed that stars associated with the outer halo are Mg-poor, while Fulbright (2002) suggested such stars may have anomalous kinematic properties. Nissen & Schuster (2010) suggested these Mg-poor stars are probably accreted from dwarf spheroidal (dSph) galaxies since similar Mg-deficient phenomena have been found in present-day dSph galaxies (Tolstoy et al. 2009). Aoki et al. (2014) proposed that first-generation very massive stars would lead to metal-poor stars that form with low [Mg/Fe]. The abundance patterns of several known extremely Mg-poor stars were reanalyzed by comparing with SN Ia models (Ivans et al. 2003). The comparison indicated that a simple combination of the yields of SN II and SN Ia could not explain the overall abundance patterns of these anomalous stars. Although the origin of these Mg-poor stars is still not understood, their unique abundance patterns suggest that they possess different nucleosynthesis histories than the majority of Galactic metal-poor stars.

Since only a small sample of Mg-poor stars has been identified through high-resolution spectroscopy, more such stars should be found and studied to gain a better understanding of their origin. However, it is not feasible to obtain high-resolution stellar spectra of large samples within the Milky Way to search for Mg-poor stars. Surveys with low-resolution spectra give us the chance to increase the sample size of such stars. In a previous work, we presented a method to select Mg-poor metal-poor stars from low-resolution SDSS spectra based on a spectral matching technique (Xing & Zhao 2014). In this paper, we use a similar method to select Mg-poor stars from the data provided by the Large Sky Area Multi-Object Fiber Spectroscopic Telescope (LAMOST; also known as the Guo Shou Jing Telescope) and report our discovery of 15 candidate Mg-poor stars from LAMOST Data Release 2 (DR2).

2 THE DATA

2.1 LAMOST DR2 Data

The LAMOST general survey is a spectroscopic survey that began regular observations in September 2012. LAMOST is a quasi-meridian reflecting Schmidt telescope (Cui et al. 2012) with an effective aperture of 4 m. The telescope is equipped with 16 spectrographs, each of which is connected to 250 fibers for acquiring low-resolution ($R \sim 1800$) spectra over the wavelength range 3700–9000 Å. The LAMOST regular survey (Zhao et al. 2006, 2012; Liu et al. 2015) finished the second year observation goals in June 2014 and obtained more than 3 million stellar spectra. These spectra, together with 800 000 stellar spectra observed during the pilot survey, have been released as DR2[1] of the LAMOST survey.

The raw data were reduced by the standard LAMOST pipeline (Luo et al. 2012), including a combination of the blue (3700–5900 Å) and red (5700–9000 Å) arms of the spectra, flat-fielding, wavelength calibration and sky background subtraction. The standard pipeline estimates the radial velocity (RV) based on cross-correlation with the ELODIE spectral library (Moultaka et al. 2004). The Université de Lyon Spectroscopic analysis software (ULySS) is used in the pipeline to estimate stellar parameters (including effective temperature, $T_{\rm eff}$, surface gravity, $\log\ g$, and metallicity, [Fe/H]) for high quality AFGK-type spectra (Wu et al. 2011). This software package is able to determine effective temperature, surface gravity and metallicity to precisions of 110 K, 0.19 dex and 0.11 dex (Gao et al. 2015) respectively. The UlySS estimates of atmospheric parameters for ~ 2.2 million stars are released as part of DR2.

[1] *http://dr2.lamost.org*

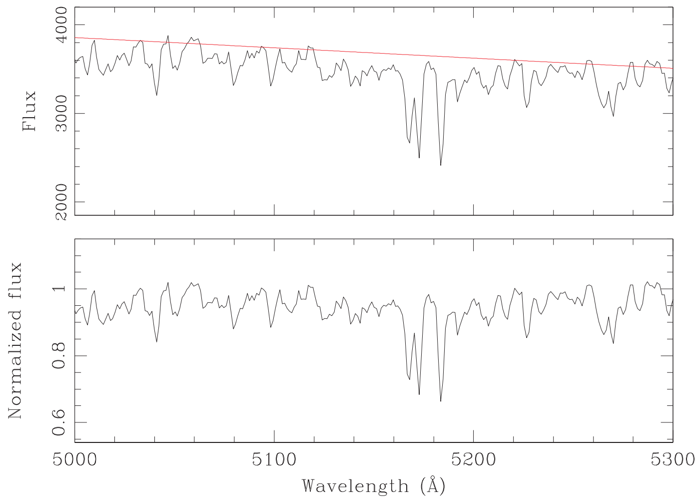

Fig. 1 In the upper panel, the observed spectrum is shown as a black line; the red line is the fitted continuum over the wavelength range of 5000–5300 Å (*color online*). The bottom panel shows the observed continuum-normalized spectrum.

2.2 Data Preprocessing

As LAMOST spectra are stored in vacuum wavelengths, we first transform the wavelength scale of the observed spectra to an air-based scale. The conversion from vacuum to air wavelengths is performed following the IAU standard given by Morton (1991). The observed spectra are then shifted to the rest frame based on the RV provided by the LAMOST standard pipeline.

In order to determine [Mg/Fe] of the LAMOST stellar spectra, we extract observed spectra over the wavelength range of 5000–5300 Å from the entire spectra. This wavelength range contains Mg $1b$ lines, which are fairly good features for determination of Mg abundance from low-resolution spectra. The spectra over the selected wavelength range are then fit to a polynomial for obtaining the pseudo-continuum.

Figure 1 shows an example of continuum determination for the LAMOST stellar spectra. The upper panel shows a fitted local continuum for an observed spectrum over the wavelength range of 5000–5300 Å. The normalized observed spectrum is shown in the bottom panel.

3 SELECTION OF CANDIDATE MG-POOR STARS

The candidate Mg-poor stars are selected based on [Mg/Fe] determined from the low-resolution spectra. We determine [Mg/Fe] by comparing the given observed spectrum to a set of synthetic spectra at fixed stellar atmospheric parameters ($T_{\rm eff}$, $\log g$ and [Fe/H]), and various [Mg/Fe] with $-0.5 \leq$ [Mg/Fe] $\leq +0.8$ in steps of 0.1 dex. The [Mg/Fe] corresponding to the minimum χ^2 is then adopted as the measured [Mg/Fe] for the given observed spectrum.

3.1 Template Spectra

The NEWODF ATLAS9 model atmospheres (Castelli & Kurucz 2003) are used to generate synthetic spectra for the spectral matching process. These models are computed under the assumption of no overshooting and local thermodynamic equilibrium (LTE). The grids of atmospheric models with α-enhancements ([α/Fe] = +0.4) and non α-enhancements ([α/Fe] = 0.0) are provided by

Castelli's website[2]. We choose to use the α-enhanced models to generate synthetic spectra with [Mg/Fe] $\geq +0.4$. The non α-enhanced models are adopted for generating synthetic spectra with [Mg/Fe] $< +0.4$. Therefore, we use linear interpolation of the logarithm of each atmospheric variable to generate two model atmospheres (α-enhanced and non α-enhanced model atmospheres) for a given combination of $T_{\rm eff}$, log g and [Fe/H]. Note that [Mg/Fe] of the majority of our synthetic spectra are not consistent with [α/Fe] ratios of the model atmospheres that are used to generate them. Hence, we performed some comparisons between synthetic spectra generated with α-enhanced and non α-enhanced model atmospheres with the same atmospheric parameters and chemical abundances. The results showed that the variation of [α/Fe] ratios for model atmospheres only results in a minimal difference in the flux of the synthetic spectra at a resolving power $R = 1800$. Thus, the differences in [α/Fe] between model atmospheres and generated synthetic spectra will not raise spurious detections of Mg-poor stars in our research.

After obtaining the desired stellar model atmospheres, we use the SPECTRUM spectral synthesis package (Gray & Corbally 1994) to generate a set of synthetic spectra covering $-0.5 \leq$ [Mg/Fe] $\leq +0.8$, in steps of 0.1 dex, at the given ($T_{\rm eff}$, $\log g$ and [Fe/H]). Considering that microturbulence has a minimal effect on spectral features of low-resolution spectra, a microturbulence of 2 km s^{-1} is adopted for each synthetic spectrum. All synthetic spectra range from 5000 to 5300 Å with a resolving power of $R = 1800$. SPECTRUM carries out this computation under the assumptions of LTE, along with the solar elemental abundances from Grevesse & Sauval (1998). Kurucz line lists[3] are employed by SPECTRUM for synthesizing template spectra.

3.2 Chemical Abundance Analysis

For a given observed spectrum, we use stellar atmospheric parameters ($T_{\rm eff}$, $\log g$ and [Fe/H]) delivered by the LAMOST DR2 catalog to generate the full set of synthetic spectra covering $-0.5 \leq$ [Mg/Fe] $\leq +0.8$, in steps of 0.1 dex. A χ^2-minimization scheme is performed by computing the difference between the observed and synthetic spectrum. As a preprocessing step, the observed spectrum has been shifted to a zero-velocity rest frame using RV determined by the LAMOST standard pipeline. Since wavelength offset has a direct impact on the accuracy of the χ^2, we seek to reduce the uncertainties in the calculation of χ^2 due to errors in the measured RV. The LAMOST DR2 catalog provides uncertainty in the measured RV for each spectrum. Thus, we compute χ^2 for a sequence of radial velocity shifts based on the given uncertainty and adopt the χ^2 at the minimum of the array as the best χ^2 value for the corresponding synthetic spectrum. Then we find the best-matching synthetic spectrum by minimizing χ^2 between the target flux and the synthetic flux. The [Mg/Fe] of the best-matching synthetic spectrum is adopted for the observed target. This is the [Mg/Fe] ratio determined by using the usual χ^2 minimization method.

In order to improve the accuracy of the measured [Mg/Fe], we perform an additional calculation based on the above data. The minimum χ^2 is determined by fitting a third order polynomial to the distribution of χ^2 versus [Mg/Fe]. We adopt the [Mg/Fe] corresponding to the minimum χ^2 as the best-fit value for the observed target. The [Mg/Fe] ratios measured by this additional approach are more accurate than those from the usual χ^2 minimization technique. Hence, we choose the latter measured [Mg/Fe] as the final result. However, there are some cases where no minimum χ^2 is found. In such cases, we adopt the former measurements.

Figure 2 provides an example of determining [Mg/Fe] for a given star with atmospheric parameters ($T_{\rm eff}$, $\log\ g$, [Fe/H]) = (6000, 4.0, –1.45). The filled circles show the observed spectrum; the black lines are the set of synthetic spectra corresponding to $-0.5 \leq$ [Mg/Fe] $\leq +0.2$ in steps of 0.1 dex; the red-dashed line is the synthetic spectrum generated with the final adopted [Mg/Fe] = -0.39.

[2] *http://wwwuser.oats.inaf.it/castelli/grids.html*
[3] *http://kurucz.harvard.edu*

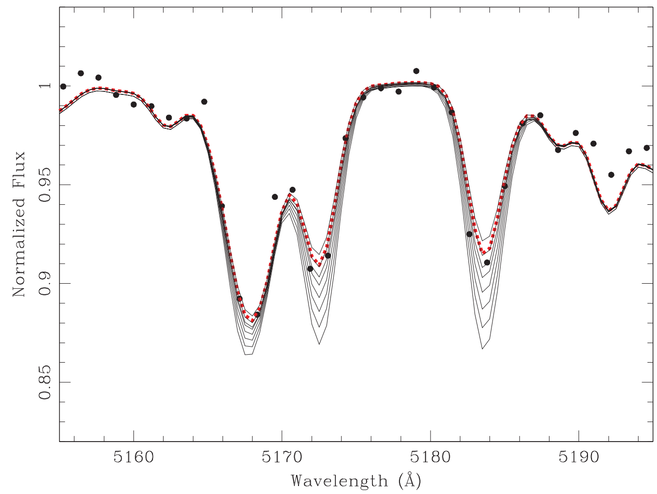

Fig. 2 An example of determining [Mg/Fe] for a given star with atmospheric parameters ($T_{\rm eff}$, $\log\ g$, [Fe/H]) = (6000, 4.0, -1.45). The filled circles show the observed spectrum. The black lines are the set of synthetic spectra corresponding to $-0.5 \leq$ [Mg/Fe] $\leq +0.2$ in steps of 0.1 dex. The red-dashed line is the synthetic spectrum generated with the final adopted [Mg/Fe] = -0.39.

4 APPLICATION AND RESULTS

We extracted $\sim 60\,000$ high quality (S/N > 50) stellar spectra with atmospheric parameters in the range of $T_{\rm eff}$ = [5500, 6500] K and [Fe/H] = [-2.4, $+0.5$] from the catalog of LAMOST DR2 AFGK-type stars. Then, these spectra were shifted to a zero-velocity rest frame and normalized following the procedures described in Section 2.2. Their [Mg/Fe] ratios were determined from the normalized observed spectra by using our χ^2 minimization method. The distribution of the [Mg/Fe] ratios versus [Fe/H] is shown in Figure 3 for all of the sample stars. We focus on finding Mg-poor ([Mg/Fe] < 0.0) and metal-poor ([Fe/H] < -0.75) stars in this research. Although candidate Mg-poor metal-poor stars can be directly selected from the sample based on the adopted [Mg/Fe], we seek to eliminate spurious detections of Mg-poor stars by checking effects of errors in $T_{\rm eff}$ and $\log\ g$ on determination of [Mg/Fe]. The [Mg/Fe] of the Mg-poor metal-poor candidates were recalculated by varying $T_{\rm eff}$ and $\log\ g$ based on the uncertainties provided by the LAMOST pipeline. If the [Mg/Fe] remain below the solar value in this process, the target would be considered as the final Mg-poor metal-poor candidate. As shown in Figure 3, 15 Mg-poor star candidates (red filled squares) are selected from our sample. The atmospheric parameters and abundances of these candidates are summarized in Table 1. They all possess sub-solar [Mg/Fe] ratios in a low metallicity range, suggesting large scatters of [Mg/Fe] may exist in this metallicity regime. In Figure 3, we compare our results to the [Mg/Fe] ratios of stars in nearby dSph galaxies (Koch & McWilliam 2008; Starkenburg et al. 2013; Letarte et al. 2010; Aoki et al. 2009; Shetrone et al. 2001). Most of these metal-poor dSph stars exhibit sub-solar values for [Mg/Fe] that are similar to those of our Mg-poor metal-poor star candidates. They may share a common explanation for their abnormal [Mg/Fe] and our Mg-poor metal-poor star candidates may have originated from dSph systems associated with the Milky Way (MW). We also note that these values of [Mg/Fe] seem to be underestimated by about 0.1 dex compared to the result from high-resolution spectroscopic analysis (Venn et al. 2004) near solar metallicity. This offset may be caused by errors in atmospheric parameters. As we have considered effects of errors in atmospheric parameters on selection of Mg-poor metal-poor candidates, this offset will not result in spurious detections of Mg-poor metal-poor stars.

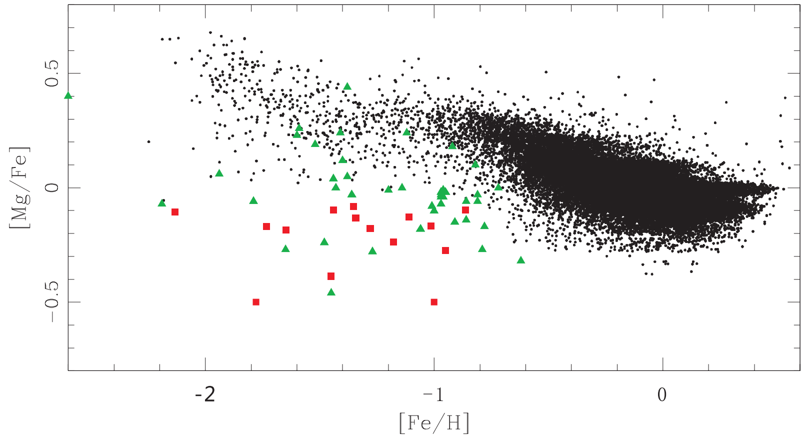

Fig. 3 The abundance ratio [Mg/Fe] as a function of [Fe/H]. The candidates are shown as red filled squares and other stars in our sample are represented by black filled circles. Stars within nearby dSph galaxies (Koch & McWilliam 2008; Starkenburg et al. 2013; Letarte et al. 2010; Aoki et al. 2009; Shetrone et al. 2001) are shown as green filled triangles.

Table 1 Candidates of Mg-poor Stars

ID	$T_{\rm eff}$	log g	[Fe/H]	RV (km s^{-1})	[Mg/Fe]
LAMOST J0049+0405	6121	4.09	−1.44	−127.54	−0.10
LAMOST J1139+5653	6353	3.84	−1.00	−6.23	−0.50
LAMOST J0709+4239	5981	3.97	−1.65	139.77	−0.19
LAMOST J1924+4145	6000	4.00	−1.45	−324.81	−0.39
LAMOST J2313+1702	6240	4.06	−1.28	−196.03	−0.18
LAMOST J2239+1150	6040	4.02	−1.18	−250.29	−0.24
LAMOST J2327+0330	6024	4.06	−1.11	−136.81	−0.13
LAMOST J0117−0133	5976	4.02	−1.35	−177.14	−0.08
LAMOST J0420−0356	5920	3.92	−1.73	10.46	−0.17
LAMOST J0956+1020	5724	3.91	−0.95	55.31	−0.27
LAMOST J1045+0518	6123	4.04	−1.78	136.05	−0.50
LAMOST J1057+1942	5912	3.83	−2.13	−44.19	−0.11
LAMOST J1132+2036	6036	3.85	−1.34	91.55	−0.13
LAMOST J0229+0314	5994	4.07	−1.01	−119.56	−0.17
LAMOST J0922+3100	5809	4.08	−0.86	−56.05	−0.10

5 SUMMARY

We have presented a method for selecting Mg-poor metal-poor stars from the LAMOST survey by fitting the Mg 1b lines from low-resolution ($R \sim 1800$) stellar spectra. From a high quality sample, 15 candidate Mg-poor metal-poor stars were selected based on the determined [Mg/Fe]. Their abnormal [Mg/Fe] ratios indicated that they may have a different chemical enrichment history than other Galactic metal-poor stars. The typical explanation for low [Mg/Fe] ratios is that the Mg-poor stars originate from environments that were deficient in massive stars like satellite dSph galaxies associated with the MW. As similar Mg-poor stars have been found in present-day MW dSph galaxies (Shetrone et al. 2001; Sbordone et al. 2007; McWilliam et al. 2013), the Galactic Mg-poor stars may be signatures of accretion of dSph galaxies. Discoveries and studies of such type of stars will improve our understanding of the assembly history of the MW. The number of presently known Mg-poor stars remains small. Hence we will apply our selection method to much larger stellar samples from LAMOST and SDSS (Xing & Zhao 2014) in further work in order to increase the sample size.

Acknowledgements This study is supported by the National Natural Science Foundation of China (Grant Nos. 11390371, 11233004, 11303040 and U1431106). The Guo Shou Jing Telescope (the Large Sky Area Multi-Object Fiber Spectroscopic Telescope, LAMOST) is a National Major Scientific Project built by the Chinese Academy of Sciences. Funding for the project has been provided by the National Development and Reform Commission. LAMOST is operated and managed by National Astronomical Observatories, Chinese Academy of Sciences.

References

Aoki, W., Arimoto, N., Sadakane, K., et al. 2009, A&A, 502, 569
Aoki, W., Tominaga, N., Beers, T. C., Honda, S., & Lee, Y. S. 2014, Science, 345, 912
Carney, B. W., Wright, J. S., Sneden, C., et al. 1997, AJ, 114, 363
Castelli, F., & Kurucz, R. L. 2003, in IAU Symposium, 210, Modelling of Stellar Atmospheres, eds. N. Piskunov, W. W. Weiss, & D. F. Gray, 20P
Cui, X.-Q., Zhao, Y.-H., Chu, Y.-Q., et al. 2012, RAA (Research in Astronomy and Astrophysics), 12, 1197
Edvardsson, B., Andersen, J., Gustafsson, B., et al. 1993, A&A, 275, 101
Fulbright, J. P. 2002, AJ, 123, 404
Gao, H., Zhang, H.-W., Xiang, M.-S., et al. 2015, RAA (Research in Astronomy and Astrophysics), in press
Gray, R. O., & Corbally, C. J. 1994, AJ, 107, 742
Grevesse, N., & Sauval, A. J. 1998, Space Sci. Rev., 85, 161
Ivans, I. I., Sneden, C., James, C. R., et al. 2003, ApJ, 592, 906
King, J. R. 1997, AJ, 113, 2302
Koch, A., & McWilliam, A. 2008, AJ, 135, 1551
Letarte, B., Hill, V., Tolstoy, E., et al. 2010, A&A, 523, A17
Liu, X. W., Zhao, G., & Hou, J. L. 2015, RAA (Research in Astronomy and Astrophysics), 15, 1089
Luo, A.-L., Zhang, H.-T., Zhao, Y.-H., et al. 2012, RAA (Research in Astronomy and Astrophysics), 12, 1243
McWilliam, A. 1997, ARA&A, 35, 503
McWilliam, A., Wallerstein, G., & Mottini, M. 2013, ApJ, 778, 149
Morton, D. C. 1991, ApJS, 77, 119
Moultaka, J., Ilovaisky, S. A., Prugniel, P., & Soubiran, C. 2004, PASP, 116, 693
Nissen, P. E., & Schuster, W. J. 2010, A&A, 511, L10
Preston, G. W., & Sneden, C. 2000, AJ, 120, 1014
Sbordone, L., Bonifacio, P., Buonanno, R., et al. 2007, A&A, 465, 815
Shetrone, M. D., Côté, P., & Sargent, W. L. W. 2001, ApJ, 548, 592
Starkenburg, E., Hill, V., Tolstoy, E., et al. 2013, A&A, 549, A88
Stephens, A., & Boesgaard, A. M. 2002, AJ, 123, 1647
Tinsley, B. M. 1979, ApJ, 229, 1046
Tolstoy, E., Hill, V., & Tosi, M. 2009, ARA&A, 47, 371
Venn, K. A., Irwin, M., Shetrone, M. D., et al. 2004, AJ, 128, 1177
Wu, Y., Luo, A.-L., Li, H.-N., et al. 2011, RAA (Research in Astronomy and Astrophysics), 11, 924
Xing, Q. F., & Zhao, G. 2014, ApJ, 790, 33
Zhao, G., Chen, Y.-Q., Shi, J.-R., et al. 2006, ChJAA (Chin. J. Astron. Astrophys.), 6, 265
Zhao, G., Zhao, Y.-H., Chu, Y.-Q., Jing, Y.-P., & Deng, L.-C. 2012, RAA (Research in Astronomy and Astrophysics), 12, 723